Investigation of Electrode Erosion Mechanism of Multi-Phase AC Arc by High-Speed Video Camera

M Tanaka, T Ikeba, Y Liu, S Choi and T Watanabe
Dept. Environmental Chemistry and Engineering, Tokyo Institute of Technology
Yokohama, Kanagawa 226-8502, Japan

E-mail: mtanaka@chemenv.titech.ac.jp

Abstract. A multi-phase AC arc has been applied to the glass melting technology. However, the electrode erosion is one of the most considerable issues to be solved. In order to investigate the erosion mechanism of the multi-phase AC arc, the combination of the high-speed video camera and the band-pass filters was introduced to measure the electrode temperature. Results indicated the tip temperature of the electrode surface in the 12-phase arc was lower than that in the 2-phase arc, while erosion rate in 12-phase arc was higher than that in the 2-phase arc. Furthermore, the dynamic behaviour of the vapours in the arc was investigated by using the same high-speed camera system. The tungsten electrode mainly evaporates at the anodic period during AC cycle. The oxygen concentration in the arc increases with larger number of the phases, resulting in the higher erosion rate in the 12-phase arc.

1. Introduction

The glass industry is a large global industry that annually produces more than 100 million tons of glass products such as sheet glass, container glass, fiber glass, optical glass, and so on. Most glass has been produced by typical Siemens-type melter fired in air with heavy oil or natural gas as the fuel. This type of melter has been used for more than 140 years because of its superior large-scale performance and continuous melting system. In the air-fuel fired furnace, the heat transfer from above burner flame to glass melt is so low that the conventional melting technology is energy intensive and time consuming, especially in the melting and the refining processes. With the rapid growth of glass usage and the increased energy and environment issues, it is crucial to develop a new glass melting technology.

An innovative in-flight glass melting technology with thermal plasmas was developed to solve the above problems [1-3]. The granulated raw material with small diameter is injected into thermal plasmas and the powders contact fully with the plasma and/or burner flame. The high heat-transfer and temperatures of the plasma will melt the raw materials quickly. In addition, the decomposed gases of carbonates are removed during the in-flight treatment to reduce the refining time considerably. Compared with the traditional glass production, the total vitrification time is evaluated as only 2-3 h at the same productivity as the fuel-fired melter.

Arc plasmas as an energy source with high energy efficiency have been applied to the in-flight glass production. In particular, the multi-phase AC arc is one of the most suitable heat sources for the in-flight glass melting because it possesses many advantages such as high energy efficiency, large plasma volume (about 100 mm in diameter), low velocity (5-20 m/s) [4, 5]. In spite of the recent experimental efforts [6, 7], the multi-phase AC arc remains to be explored. In particular, the electrode

erosion is one of the most considerable issues for the practical use of the multi-phase arc in glass melting process, because it determines the electrode lifetime and the purity of the products.

The objective of the present study was to investigate the erosion mechanism of the electrode in the multi-phase AC arc. Combination of the two-colour pyrometry and the high-speed camera observation was applied to measure the temperature of the electrode on the millisecond time scale. Furthermore, the high-speed observations of the vapours in the arc were conducted to understand the dynamic behaviour of the metal vapour in the arc, which would be strongly related to the erosion phenomena. In the present work, the electrode temperature and the dynamic behaviour of the vapours in the arc were compared between the 2-phase and 12-phase arcs.

2. Experimental Procedure

2.1. Experimental setup

The schematic diagram of the experimental setup is shown in figure 1. It consisted of 12 electrodes, arc chamber, and AC power supply. The electrodes were symmetrically arranged by the angle of 30 degree and were divided into two layers, upper six and lower six electrodes. The electrodes were made of tungsten (98wt%) and thoria (2wt%) with diameter of 6 mm. City water was used to cool the electrodes at 3 slpm of water flow rate for each electrode. 99.99% argon was injected around the electrode at 5 slpm of gas flow rate to prevent them from the oxidation. Because the multi-phase arc discharge was generated under the atmospheric air except of above mentioned argon, main plasma forming gas was air. 24 Sets of arc welding transformers with single-phase AC (DAIHEN B-300, Japan) were used to generate the multi-phase AC arc discharge. The more detail about the power supply was explained in the previous report [6, 7]. In the present work, arc current was adjusted at AC 100 A for each electrode. The electrode erosion rates were evaluated from the weight difference of the electrode before and after experiments.

The applied voltage between each electrode and the neutral point of the coil of the transformer can be calculated by the following equation:

$$V_i^N = V_m^N \sin\left[\omega t - 2\pi(i-1)/12\right], \text{(i = 1, 2…12)} \tag{1}$$

where V_i^N indicates the applied non-load voltage for each electrode number i and V_m indicates the amplitude of the non-load voltage (about 220 V). The voltage was applied to only electrode No. 1 and No. 7 for the 2-phase arc discharge. In the case of the 12-phase arc discharge, the voltage was applied to electrode No. 1, 2…12.

2.2. Temperature measurements by high-speed video camera

According to the Wien's approximation of Planck's law, the spectrum of thermal radiation from a blackbody is used to determine the electrode temperature at the applied wavelengths. A real body that emits less thermal radiation than the blackbody has surface emissivity ε less than 1. Since the emissivity is unknown for many applications, the grey body assumption $\varepsilon(\lambda_1) = \varepsilon(\lambda_2)$ is used where it is hypothesized that the surface emissivity is independent of wavelength.

$$TR_{\lambda 1} = K\varepsilon(\lambda_1)d^2\lambda_1^{-5}\left(e^{k2/\lambda_1 T} - 1\right)^{-1} \tag{2}$$

Based on these approximations, the electrode temperature T is obtained from the ratio of the radiation intensity,

$$T = \frac{K_2(\lambda_1 - \lambda_2)}{\lambda_1\lambda_2}\left[\ln\left(\frac{TR_{\lambda 1}}{TR_{\lambda 2}}\right) + 5\ln\left(\frac{\lambda_1}{\lambda_2}\right)\right]^{-1} \tag{3}$$

where K_2 is the second radiation constant in Plank's law which value is 1.439×10^{-2} m·K, $TR_{\lambda1}$ and $TR_{\lambda2}$ are the thermal radiations emitted by the electrode at λ_1 and λ_2, respectively.

Spectroscopic measurements (iHR550, Horiba Jobin Yvon) were conducted to determine appropriate wavelengths for two-colour radiations. High-speed video camera (FASTCAM SA-5, Photron) with the band-pass filter system was used to measure the radiation intensities as shown in figure 2. Electrode temperature was then evaluated from the radiation intensities at 785 nm and 880 nm. Typical frame rate and exposure time of the measurements were 10,000 fps and 20 μs, respectively. The voltage of each electrode was recorded at 1MHz by an oscilloscope (Scope Corder DL 850, Yokogawa) synchronized with the high-speed camera.

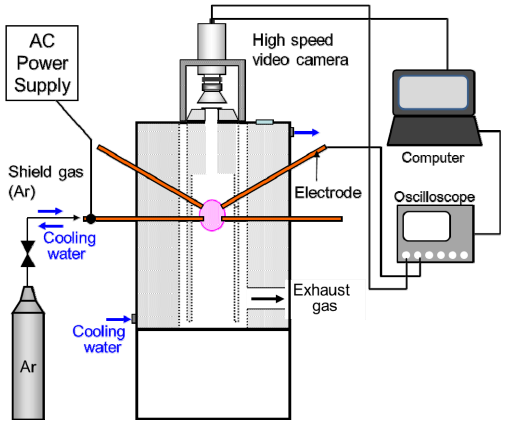

Figure 1. Schematic of the generating system of the multi-phase arc.

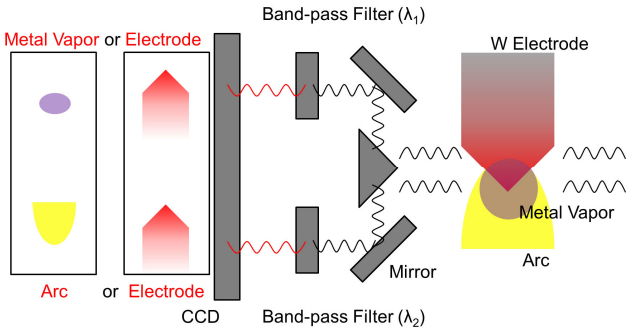

Figure 2. Schematic of the combination of the high-speed video camera and the band-pass filters.

2.3. High-speed observations of vapours in the arc

The dynamic behaviour of the vapours in the arc was investigated by using the same system with the temperature measurements. Emissions from atomic argon, oxygen, and tungsten vapours were observed at the wavelength of 738 nm, 777 nm, and 393 nm, respectively. Typical frame rate and the exposure time of the measurements were 10,000 fps and 100 μs. The voltage of each electrode was also measured at 1MHz synchronized with the high-speed camera.

3. Results and Discussion

3.1. Temperature estimation

Figure 3 shows the snapshot of the electrode obtained by the high-speed camera and the representative temperature distribution of the electrode for the 12-phase arc. The grey image indicates the arc. The temperature around the electrode tip was higher than the melting point of tungsten (3,695 K). The electrode tip temperature was estimated from the obtained temperature distributions.

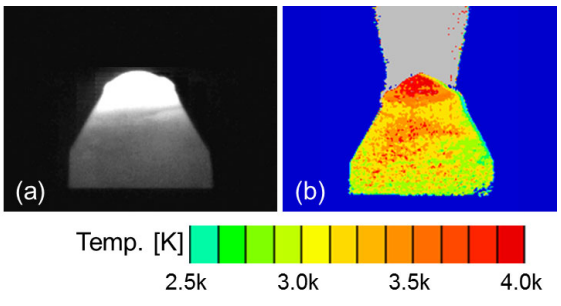

Figure 3. Snapshot of the electrode taken by the high-speed camera (a) and representative electrode temperature distribution in 12-phase AC arc (b).

Figure 4 shows the temperature variation of the electrode tip for the 2-phase and the 12-phase AC arcs in one AC cycle. Two peaks of the tip temperature were found in both cases for the 2-phase and the 12-phase arcs. These peaks originated in the peaks of the sinusoidal current waveform in AC cycle, resulting in the peak values of the heat transfer from the arc to the electrode. The temperature variation range of the 12-phase arc was smaller than that of the 2-phase arc. This could originate in the existence of the multiple arcs at the same time in the case of the multi-phase arc, while the only single arc exists in the case of the 2-phase arc.

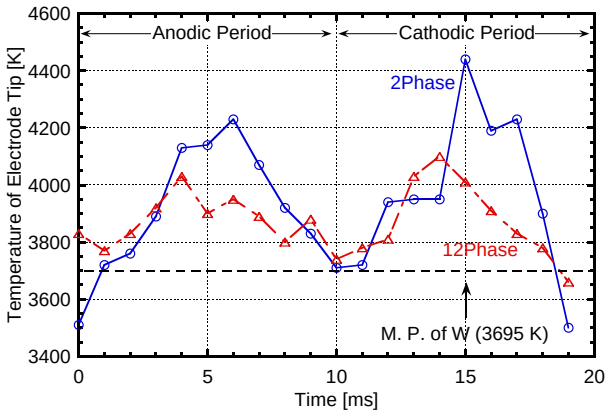

Figure 5. Temperature variation of the electrode tip for the 2-phase and the 12-phase arcs in one cycle.

Table 1 shows the comparison of the maximum temperature of the electrode tip and the erosion rate between the 2-phase and the 12-phase arcs. Maximum temperature in 12-phase arc was lower than that in the 2-phase arc, although the erosion rate for each electrode in the 12-phase arc was larger than that in the 2-phase arc. In general the temperature is one of the most crucial factors on the material evaporation, thus this relationship between the above maximum temperature and the erosion rate is unreasonable. This will be discussed in the next section.

Table 1. Maximum temperature of the electrode tip and the erosion rate per each electrode for the 2-phase and the 12-phase arcs.

	Maximum tip temperature in one cycle [10^3 K]	Erosion rate for each electrode [mg/min]
2-phase arc	4.4	0.31
12-phase arc	4.1	1.64

3.2. High-speed observations of the vapours in the arc

In order to understand the reason for the higher erosion rate in the 12-phase arc, high-speed observations of the vapours in the arc were conducted. Especially, the dynamic behaviour of the tungsten vapour was investigated to observe the evaporation of the electrode directly. Then, the oxygen entrainments into the arc were compared between the 2-phase and the 12-phase arcs. This is because the tungsten oxide formation on the electrode leads to sever erosion due to the lower melting point of tungsten oxide than metal tungsten [8, 9].

Figure 5 shows the arc current waveform synchronized with the high-speed observations. Figure 6 shows the snapshots of the high-speed video images for tungsten and argon during one cycle. The indicated time in figure 6, such as 1 ms, corresponds to the time in figure 5. The electrode was at the anodic period in the first half period, while that was at the cathodic period in the second half period. Importantly, the strong emissions from the tungsten vapours were observed in the 12-phase arc only at the anodic period. The tungsten electrode started to evaporate just after the peak top of the arc current at 5 ms in the anodic period. This is because the larger heat transfer to the electrode from the arc at the anodic period compared to the cathodic period, resulting from the electron condensation. These results indicate that the tungsten electrode was mainly evaporated at the anodic period.

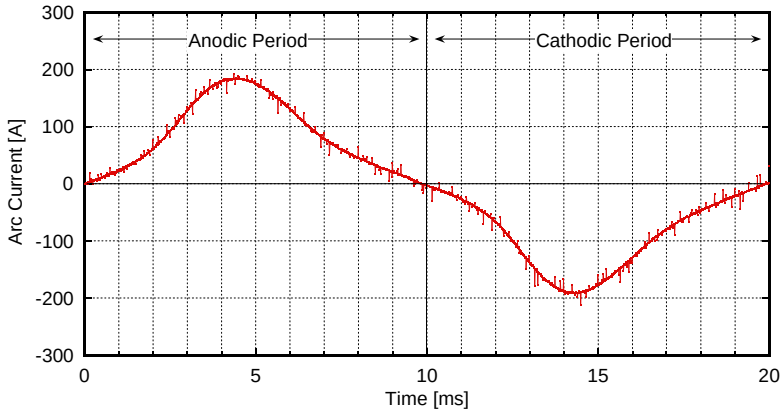

Figure 5. The waveforms of the arc current synchronized with the high-speed images shown in figure 5.

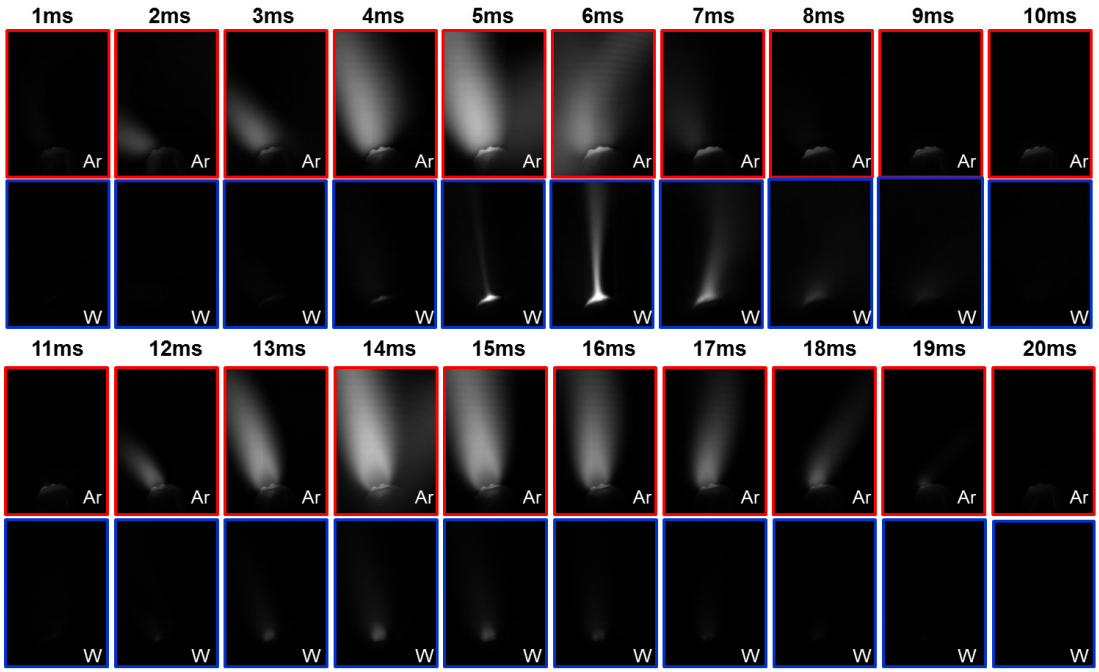

Figure 6. The snapshots of the high-speed video images for tungsten and argon during one cycle.

Figure 7 (a) and (b) shows the representative snapshots of the high-speed video images for argon and oxygen at anodic period. In order to evaluate the number density of oxygen qualitatively, the relative intensity of emissions from oxygen to that from argon was calculated. Figure 7 (c) shows the relative intensity distributions for the 2-phase and the 12-phase arcs. The relative intensity of oxygen to argon in the 12-phase is higher than that in the 2-phase arc. This result indicates that the oxygen concentration in the 12-phase arc is higher than that in the 2-phase arc. In fact, the arc-spot motion in the 12-phase is more widely distributed compared to the 2-phase arc [6]. Therefore, the ambient oxygen gas is more easily entrained with the increase of the number of the phases, resulting in the decrease of the melting point due to the oxidation of the tungsten. Consequently, the electrode erosion in the 12-phase arc was severe compared to the 2-phase arc. To reduce the oxygen entrainment must be important to apply the multi-phase AC arc to industrial field.

Further experimental studies enable us to understand the electrode erosion mechanism of the multi-phase AC arc and currently under investigation by using the high-speed camera system.

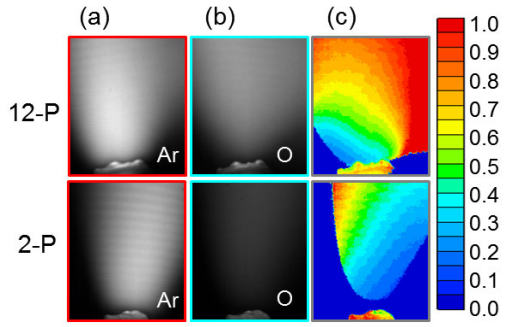

Figure 7. The representative snapshots of the high-speed video images for argon (a) and oxygen (b) and relative intensity distributions of the emissions from oxygen to that from argon (c).

4. Conclusions

The erosion mechanism of the tungsten electrode in the multi-phase AC arc was investigated by using the high-speed video camera combined with the band-pass filters. The obtained results are as follows.

(1) The electrode temperature was successfully measured on the millisecond time scale. Results indicated that the tip temperature in the 12-phase arc was lower than that in the 2-phase arc.

(2) The high-speed observations of the vapours in the arc were conducted to observe the metal vapour during the arc and the effect of the oxygen entrainments into the arc. The erosion of tungsten electrode was visually observed under anodic period with higher oxygen concentration.

(3) The ambient oxygen gas is more easily entrained into the arc with increasing the number of phases, resulting from the wider distributed arc-spot motion. Thus, the erosion rate increases with the number of the phases.

Acknowledgments

The financial support provided by the Strategic Development of Energy Conservation Technology Project of NEDO (New Energy and Industry Technology Development Organization, Japan) is gratefully acknowledged.

References

[1] Yao Y, Watanabe T, Yano T, Iseda T, Sakamoto O, Iwamoto M and Inoue S 2008 An innovative energy-saving in-flight melting technology and its application to glass production *Sci. Technol. Adv. Mater.* **9** 025013

[2] Yao Y, Yatsuda K, Watanabe T, Funabiki F and Yano T 2008 Investigation on in-flight melting behavior of granulated alkali-free glass raw material under different conditions with 12-phase AC arc *Chem. Eng. J.* **144** 317-23

[3] Watanabe T, Yatsuda K, Yao Y, Yano T and Matsuura T 2010 Innovative in-flight glass-melting technology using thermal plasmas *Pure Appl. Chem.* **82** 1337-51

[4] Liu Y, Tsuruoka Y, Tanaka M, Ichihashi T, Yano T and Watanabe T 2011 In-flight melting behavior of different glass raw materials by hybrid heating of twelve-phase AC arc with oxygen burner *Thin Solid Films* **519** 7005-8

[5] Tanaka M, Tsuruoka Y, Liu Y and Watanabe T 2011 Investigation on in-flight melting behaviour of granulated glass raw material by multi-phase AC arc plasma and hybrid plasma *IOP Conf. Ser.: Mater. Sci. Eng.* **18** 112010

[6] Tanaka M, Tsuruoka Y, Liu Y, Matsuura T and Watanabe T 2011 Investigation of multiphase AC arc behaviour by high-speed video observation *IEEE Trans. Plasma Sci.* **39** 2904-5

[7] Tanaka M, Tsuruoka Y, Liu Y, Matsuura T and Watanabe T 2011 Stability analysis of multi-phase AC arc discharge for in-flight glass melting *Current Appl. Phys.* **11** S35-9

[8] Ogawa Y, Matsuda J and Morita T 2004 Effect of ambient pressure on arc-electrode behaviour *Proc. ISOPE*, 171-8

[9] Ogawa Y 2011 High speed imaging technique Part 1 – high speed imaging of arc welding phenomena *Sci. Technol. Weld. Join.* **16**(1) 33-43